

1N-32

26381

P-19

# NASA Technical Memorandum 102729

## Transverse Electric Scattering Widths for Strips - Fourier Transform Technique

C. R. Cockrell  
S. D. Harrah  
F. B. Beck

(NASA-TM-102729) TRANSVERSE ELECTRIC SCATTERING WIDTHS FOR STRIPS-FOURIER TRANSFORM TECHNIQUE (NASA) 19 p CSCL 20N

N91-27401

Unclass  
G3/32 0026381

June 1991



National Aeronautics and Space Administration

Langley Research Center  
Hampton, Virginia 23665-5225

100

100

# TRANSVERSE ELECTRIC SCATTERING WIDTHS FOR STRIPS - FOURIER TRANSFORM TECHNIQUE

## ABSTRACT

A technique which is based on Fourier transformations is introduced for predicting scattering widths. For a strip it is shown that explicit determination of the linear current density is not necessary for both bistatic and monostatic scattering width calculations. Comparisons of the predictions of the technique in this paper are made with the integral equation (IE) technique predictions, which do require explicit evaluations of linear current densities.

## INTRODUCTION

The most commonly used methods for predicting the scattering widths (SW) of scattering objects are physical optics (PO), integral equation (IE), and geometrical theory of diffraction (GTD) [1-6]. The PO technique predicts the scattered fields quite well for objects large in wavelengths, particularly in the backscattered direction and for normally incident fields. The IE technique requires the solution of an integral equation for the induced current density on the scattering object. Numerical techniques such as the method of moments (MOM) are used to solve for the current density. The IE solution is usually referred to as the exact solution. However, for bodies which are large in terms of wavelengths, the solution can be quite time consuming, and therefore, the IE technique is usually restricted to bodies a few wavelengths in size. On the other hand, the GTD high frequency technique is more applicable to scattering bodies which are large in wavelengths. It is an extension of geometrical optics and accounts for finite edge effects using diffraction theory.

In this paper a different approach for solving scattered electromagnetic fields from flat strips is introduced. Even though the strip model may be unrealistic, it provides a useful geometry for verification of the technique since a wealth of computational data is readily available for comparison [5]. The technique is based on applications of the Fourier transform of the tangential electric field in the plane containing the strip and the current density on the strip. In general, once the current density is determined, the far fields are found from the radiation integral. The scattering width for a strip is then determined from these scattered far fields. Also, only the case for which the incident transverse electric field (TE to the infinite length of the strip) illuminates the strip is investigated. The results using this technique are then compared to results obtained by the IE technique.

TE FOURIER TRANSFORM TECHNIQUE FORMULATION  
WITH PLANE WAVE INCIDENCE ON A STRIP

A plane wave with wave number  $k$ , polarized in the  $x$ - $y$  plane, and represented as  $\mathbf{E} = [\hat{x}\cos\theta_1 - \hat{y}\sin\theta_1]e^{jk[x\sin\theta_1 + z\cos\theta_1]}$  is assumed incident at an angle  $\theta_1$  on a perfecting conducting strip of width  $a$  located in the  $z = 0$  plane (see fig.1). The incident electric field induces a linear electric current density  $J_x$ , which in turn radiates the scattered fields. Once  $J_x$  is known, the scattered field is readily found from the radiation integral.

Since only the  $x$  component of the electric field induces a linear current density on the strip, the  $x$  component of the magnetic vector potential is written as

$$A_x(x, z) = \frac{\mu}{4\pi} \iint_{\text{strip}} J_x(x', y') \frac{e^{-jkR}}{R} dx' dy' \quad (1)$$

where  $R = \sqrt{(x-x')^2 + (y-y')^2 + z^2}$  and  $\mu$  is the permeability of free space. Performing the  $y'$  integration (assuming  $J_x$  is independent of  $y'$ ),

$$A_x(x, z) = -j \frac{\mu}{4} \int_{-\frac{a}{2}}^{\frac{a}{2}} J_x(x') H_0^{(2)} \left( kv\sqrt{(x-x')^2 + z^2} \right) dx' \quad (2)$$

where  $H_0^{(2)}()$  is the zero-th order Hankel function of the second kind. From one of Maxwell's curl equations, the  $y$  component of the  $H$  field can be written as

$$H_y(x, z) = -j \frac{1}{4} \int_{-\frac{a}{2}}^{\frac{a}{2}} J_x(x') \frac{\partial}{\partial z} H_0^{(2)} \left( kv\sqrt{(x-x')^2 + z^2} \right) dx' \quad (3)$$

Also, since  $H_y$  satisfies the wave equation

$$\frac{\partial^2 H_y}{\partial x^2} + \frac{\partial^2 H_y}{\partial z^2} + k^2 H_y = 0 \quad (4)$$

it can be expressed in terms of spectrum solutions as

$$\left. \begin{aligned} H_y^+(x, z) &= \frac{1}{2\pi} \int_{-\infty}^{\infty} G^+(k_x) e^{-jk_x x} e^{-jk_z z} dk_x, & z > 0 \\ H_y^-(x, z) &= \frac{1}{2\pi} \int_{-\infty}^{\infty} G^-(k_x) e^{-jk_x x} e^{jk_z z} dk_x, & z < 0 \end{aligned} \right\} \quad (5)$$

where the G's are the spectrum functions and

$$k_z = \left\{ \begin{array}{ll} \sqrt{k^2 - k_x^2}, & k_x^2 < k^2 \\ -j \sqrt{k_x^2 - k^2}, & k_x^2 > k^2 \end{array} \right\} \quad (6)$$

In equation (5), the superscripts + and - denote the regions  $z > 0$  and  $z < 0$ , respectively.

Under the assumption that the strip is now replaced with a linear current density  $J_x$ , the boundary conditions on the tangential field components in the  $z = 0$  plane are applied. The tangential H field is discontinuous by the amount of linear current density flowing on the region which was occupied by the strip; that is,

$$J_x = -H_y^+ + H_y^- \quad (7)$$

Substituting equation (5) into equation (7) for  $z = 0$ , the linear current density becomes

$$J_x = \frac{1}{2\pi} \int_{-\infty}^{\infty} \left[ -G^+(k_x) + G^-(k_x) \right] e^{-jk_x x} dk_x \quad (8)$$

The tangential electric field at  $z = 0$  is continuous. Therefore, from Maxwell's curl equation

$$\mathbf{E} = \frac{1}{j\omega\epsilon} \nabla \times \mathbf{H} \quad (9)$$

the continuity of  $E_x$  yields

$$\frac{1}{j2\pi\omega\epsilon} \int_{-\infty}^{\infty} G^-(k_x) (jk_z) e^{-jk_x x'} dk_x = \frac{1}{j2\pi\omega\epsilon} \int_{-\infty}^{\infty} G^+(k_x) (-jk_z) e^{-jk_x x'} dk_x \quad (10)$$

where  $\epsilon$  is the permittivity of free space. The solution of equation (10) is

$$G^-(k_x) = -G^+(k_x) \quad (11)$$

Substituting equation (11) into equation (8), the linear current density becomes

$$J_x(x') = -\frac{2}{2\pi} \int_{-\infty}^{\infty} G^+(k_x) e^{-jk_x x'} dk_x \quad (12)$$

Its inverse Fourier transform is

$$-2G^+(k_x) = \int_{-\infty}^{\infty} J_x(x') e^{jk_x x'} dx' \quad (13)$$

with the understanding that  $J_x(x')$  is zero outside the strip width.

For the approach in this study, it is necessary to express the magnetic vector potential component in terms of a Fourier spectrum representation; therefore, let

$$J_{x\delta}(x') = I \delta(x' - x'') \quad (14)$$

where  $I$  is a current and  $\delta(x' - x'')$  is a delta function located at a general point  $x''$  on the strip [1]. The subscript  $\delta$  is used to denote the solution for an impulsive linear current density. From equation (3)

$$H_{y\delta} = -j \frac{1}{4} I \frac{\partial}{\partial z} H_0^{(2)} \left( k \sqrt{(x - x'')^2 + z^2} \right) \quad (15)$$

and from equation (13)

$$-2G_{\delta}^+(k_x) = I e^{jk_x x''} \quad (16)$$

Using equation (16), the first equation of equation (5) can be written as

$$H_{y\delta} = \frac{1}{2\pi} \int_{-\infty}^{\infty} \left[ -\frac{I e^{jk_x x''}}{2} \right] e^{-jk_x x} e^{-jk_z z} dk_x \quad (17)$$

Equating equations (15) and (17)

$$\frac{\partial}{\partial z} H_0^{(2)} \left( k \sqrt{(x - x'')^2 + z^2} \right) = \frac{1}{j\pi} \int_{-\infty}^{\infty} e^{-jk_x(x-x'')} e^{-jk_z z} dk_x \quad (18)$$

The solution of equation (18) is found by integrating over  $z$ ; therefore,

$$H_0^{(2)} \left( k \sqrt{(x - x'')^2 + z^2} \right) = \frac{1}{\pi} \int_{-\infty}^{\infty} \frac{1}{k_z} e^{-jk_x(x-x'')} e^{-jk_z z} dk_x \quad (19)$$

The magnetic vector potential component from equation (2) becomes

$$A_x(x, z) = -j \frac{\mu}{4\pi} \int_{x' = -\frac{a}{2}}^{\frac{a}{2}} J_x(x') \int_{k_x = -\infty}^{\infty} \frac{1}{k_z} e^{-jk_x(x-x')} e^{-jk_z z} dk_x dx' \quad (20)$$

where the double prime on  $x$  has been changed to a single prime. The tangential electric field in terms of  $A_x$  is [5]

$$E_x(x, z) = -j\omega A_x(x, z) - j \frac{1}{\omega\mu\epsilon} \frac{\partial^2}{\partial x^2} A_x(x, z) \quad (21)$$

With equation (20) substituted into equation (21), the tangential electric field becomes

$$E_x(x, z) = - \frac{1}{4\pi\omega\epsilon} \int_{x' = -\frac{a}{2}}^{\frac{a}{2}} J_x(x') \int_{k_x = -\infty}^{\infty} k_z e^{-jk_x(x-x')} e^{-jk_z z} dk_x dx' \quad (22)$$

Interchanging the order of integration, equation (22) becomes

$$E_x(x, z) = - \frac{1}{4\pi\omega\epsilon} \int_{k_x = -\infty}^{\infty} k_z \left[ \int_{-\frac{a}{2}}^{\frac{a}{2}} J_x(x') e^{jk_x x'} dx' \right] e^{-jk_x x} e^{-jk_z z} dk_x \quad (23)$$

After rewriting equation (23) as

$$E_x(x, z) = \frac{1}{2\pi} \int_{-\infty}^{\infty} \left[ - \frac{1}{2\omega\epsilon} k_z \int_{-\frac{a}{2}}^{\frac{a}{2}} J_x(x') e^{jk_x x'} dx' \right] e^{-jk_x x} e^{-jk_z z} dk_x \quad (24)$$

the term in square brackets is defined as  $F_x(k_x)$ . Therefore,



equation (24) becomes

$$E_x(x, z) = \frac{1}{2\pi} \int_{-\infty}^{\infty} F_x(k_x) e^{-jk_x x} e^{-jk_z z} dk_x \quad (25)$$

At this point the problem is formulated as a scattering one; that is, the total tangential electric field is written as

$$E_x^T(x, z) = E_x^I(x, z) + E_x^S(x, z) \quad (26)$$

where  $E_x^I(x, z)$  is the incident field and  $E_x^S(x, z)$  is the scattered field which is assumed to be representable as equation (25). Therefore,

$$E_x^T(x, z) = E_x^I(x, z) + \frac{1}{2\pi} \int_{-\infty}^{\infty} F_x(k_x) e^{-jk_x x} e^{-jk_z z} dk_x \quad (27)$$

where

$$F_x(k_x) = -\frac{k_z}{2\omega\epsilon} \int_{-\frac{a}{2}}^{\frac{a}{2}} J_x(x') e^{jk_x x'} dx' \quad (28)$$

Since the unknown function  $J_x(x')$  appears only under the integral sign, equation (28) is an integral equation of the second kind. Such equations are often solved approximately by the method of moments where the unknown function is expressed as a sum of basis functions with unknown constants. The constants are then found through a point matching technique which requires a matrix inversion.

An approximate solution for  $J_x(x')$  is determined by a Fourier transformation inversion. At  $z = 0$  equation (27) becomes

$$E_x^T(x', 0) = \cos\theta_1 e^{jk_x x' \sin\theta_1} + \frac{1}{2\pi} \int_{-\infty}^{\infty} F_x(k_x) e^{-jk_x x'} dk_x \quad (29)$$

If the  $E_x^T(x', 0)$  were known over the complete  $z = 0$  plane, the true  $F_x(k_x)$  can be found via the inverse Fourier transform. However, the field  $E_x^T(x', 0)$  is known only over the strip ( $E_x^T = 0$ ) and not outside. As an approximation the total  $E_x^T(x', 0)$  field outside the strip is assumed to be the tangential incident field. Written in mathematical terms, the tangential electric field in the  $z = 0$  plane is

$$E_{x\alpha}^T(x', 0) = [1 - s(x')] \cos\theta_1 e^{jkx' \sin\theta_1} \quad (30)$$

where the subscript  $\alpha$  on  $E_{x\alpha}^T(x', 0)$  denotes an approximation and

$$s(x') = \begin{cases} 1 & , |x'| \leq \frac{a}{2} \\ 0 & , \text{otherwise} \end{cases} \quad (31)$$

Substitution of equation (30) into equation (29) gives

$$\frac{1}{2\pi} \int_{-\infty}^{\infty} F_{x\alpha}(k_x) e^{-jk_x x'} dk_x = -s(x') \cos\theta_1 e^{jkx' \sin\theta_1} \quad (32)$$

The inverse Fourier transform yields

$$F_{x\alpha}(k_x) = -a \frac{\sin\left(k_x + k \sin\theta_1\right) \frac{a}{2}}{\left(k_x + k \sin\theta_1\right) \frac{a}{2}} \cos\theta_1 \quad (33)$$

An approximate solution for the linear current density in equation (28) is found by a Fourier transformation of an approximate linear current density  $J_{x\alpha}(x')$ ; that is

$$\int_{-\infty}^{\infty} J_{x\alpha}(x') e^{jk_x x'} dx' = -\frac{2\omega\epsilon}{k_z} F_{x\alpha}(k_x) \quad (34)$$

The inverse Fourier transform yields

$$J_{x\alpha}(x') = \frac{1}{2\pi} \int_{-\infty}^{\infty} \left[ \frac{2\omega\epsilon}{k_z} a \frac{\sin\left(k_x + k \sin\theta_1\right) \frac{a}{2}}{\left(k_x + k \sin\theta_1\right) \frac{a}{2}} \cos\theta_1 \right] e^{-jk_x x'} dk_x \quad (35)$$

This inverse transformation produces linear current density inside and outside the strip width. Since the linear current density  $J_x(x')$  given in equation (24) flows only on the strip, it is set equal to  $J_{x\alpha}(x')$  only over the strip width; that is,

$$J_x(x') = \begin{cases} J_{x\alpha}(x') & , |x'| \leq \frac{a}{2} \\ 0 & , \text{otherwise} \end{cases} \quad (36)$$

For normal incidence ( $\theta_1 = 0$ ), equation (35) is evaluated numerically for a strip two-wavelengths wide. In figure 2, these computations are compared with the linear current density obtained by the integral equation technique which uses the method of moments. Even though the two solutions do not agree in magnitude over the complete strip, their shapes are very similar. Techniques for improving the agreement between the solutions will be investigated in future work.

## TE SCATTERING WIDTH OF A STRIP

The definition of the scattering width of a strip (object) is given as [5]

$$\sigma_{2-D} = \left\{ \begin{array}{l} \lim_{\rho \rightarrow \infty} \left[ 2\pi\rho \frac{|E^S|^2}{|E^I|^2} \right] \\ \lim_{\rho \rightarrow \infty} \left[ 2\pi\rho \frac{|H^S|^2}{|H^I|^2} \right] \end{array} \right\} \quad (37)$$

where  $\rho$  is the distance from the strip to the observation point,  $E^S, H^S$  are the scattered fields, and  $E^I, H^I$  are the incident fields. In this paper the second definition is used where the scattered H field component is given by equation (3). Explicitly performing the differentiation in equation (3), the scattered y-component H field becomes

$$H_y^S(x, z) = j \frac{k}{4} \int_{-\frac{a}{2}}^{\frac{a}{2}} J_x(x') \frac{z}{\sqrt{(x-x')^2 + z^2}} H_1^{(2)}\left(k\sqrt{(x-x')^2 + z^2}\right) dx' \quad (38)$$

where  $H_1^{(2)}()$  is the first order Hankel function of the second kind. Since scattering widths are based on far-field expressions, the square root term in equation (38) can be approximated as

$$\sqrt{(x-x')^2 + z^2} \cong \begin{cases} \rho - x' \sin\theta_s & , \text{ for phase terms} \\ \rho & , \text{ for amplitude terms} \end{cases} \quad (39)$$

where  $\theta_s$  is the scattered angle off the normal to the strip (see fig.1). For  $k(\rho - x' \sin\theta_s)$  large, the Hankel function can be written as

$$H_1^{(2)}() \cong j \sqrt{\frac{2}{\pi k \rho}} e^{-jk(\rho - x' \sin\theta_s)} e^{j\frac{\pi}{4}} \quad (40)$$

Substituting equations (39) and (40) into equation (38) with  $z = \rho \cos\theta_s$ , the total scattered H far field becomes

$$H^S \cong - \hat{y} \sqrt{\frac{k}{8\pi}} \frac{e^{-jk\rho}}{\sqrt{\rho}} e^{j\frac{\pi}{4}} \cos\theta_s \int_{-\frac{a}{2}}^{\frac{a}{2}} J_x(x') e^{jkx' \sin\theta_s} dx' \quad (41)$$

Instead of explicitly solving for the linear current density, the

integral representation given by equation (35) is substituted directly into equation (41). The order of integration is then interchanged, permitting the analytical integration over  $x'$ . This procedure greatly reduces the computational time since only a single numerical integration is now required. The total H far field is now written as

$$H^S \cong - \hat{Y} \frac{\omega \epsilon}{\pi} \sqrt{\frac{k}{8\pi}} \frac{e^{-jk\rho}}{\sqrt{\rho}} e^{j\frac{\pi}{4}} \cos\theta_s \cos\theta_1 \cdot \int_{-\infty}^{\infty} \frac{1}{k_z} \left[ a \frac{\sin\left(\frac{k_x + k \sin\theta_1}{k_x + k \sin\theta_1}\right)^{\frac{a}{2}}}{\left(\frac{k_x + k \sin\theta_1}{k_x + k \sin\theta_1}\right)^{\frac{a}{2}}} \right] \left[ a \frac{\sin\left(\frac{k_x - k \sin\theta_s}{k_x - k \sin\theta_s}\right)^{\frac{a}{2}}}{\left(\frac{k_x - k \sin\theta_s}{k_x - k \sin\theta_s}\right)^{\frac{a}{2}}} \right] dk_x \quad (42)$$

for bistatic scattering and

$$H^S \cong - \hat{Y} \frac{\omega \epsilon}{\pi} \sqrt{\frac{k}{8\pi}} \frac{e^{-jk\rho}}{\sqrt{\rho}} e^{j\frac{\pi}{4}} \cos^2\theta_1 \cdot \int_{-\infty}^{\infty} \frac{1}{k_z} \left[ a \frac{\sin\left(\frac{k_x + k \sin\theta_1}{k_x + k \sin\theta_1}\right)^{\frac{a}{2}}}{\left(\frac{k_x + k \sin\theta_1}{k_x + k \sin\theta_1}\right)^{\frac{a}{2}}} \right] \left[ a \frac{\sin\left(\frac{k_x - k \sin\theta_1}{k_x - k \sin\theta_1}\right)^{\frac{a}{2}}}{\left(\frac{k_x - k \sin\theta_1}{k_x - k \sin\theta_1}\right)^{\frac{a}{2}}} \right] dk_x \quad (43)$$

for monostatic scattering. The scattering widths for the incident H field

$$H^I = - \hat{Y} \sqrt{\frac{\epsilon}{\mu}} e^{jk_x x \sin\theta_1} e^{jk_z z \cos\theta_1} \quad (44)$$

are given as

$$\sigma_{2D}(\text{bistatic}) = \frac{k^3}{4\pi^2} \cos^2\theta_s \cos^2\theta_1 \cdot \left| \int_{-\infty}^{\infty} \frac{1}{k_z} \left[ a \frac{\sin\left(\frac{k_x + k \sin\theta_1}{k_x + k \sin\theta_1}\right)^{\frac{a}{2}}}{\left(\frac{k_x + k \sin\theta_1}{k_x + k \sin\theta_1}\right)^{\frac{a}{2}}} \right] \left[ a \frac{\sin\left(\frac{k_x - k \sin\theta_s}{k_x - k \sin\theta_s}\right)^{\frac{a}{2}}}{\left(\frac{k_x - k \sin\theta_s}{k_x - k \sin\theta_s}\right)^{\frac{a}{2}}} \right] dk_x \right|^2 \quad (45)$$

and

$$\sigma_{2D}(\text{monostatic}) = \frac{k^3}{4\pi^2} \cos^4\theta_1 \cdot \left| \int_{-\infty}^{\infty} \frac{1}{k_z} \left[ a \frac{\sin\left(\frac{k_x + k \sin\theta_1}{k_x + k \sin\theta_1}\right)^{\frac{a}{2}}}{\left(\frac{k_x + k \sin\theta_1}{k_x + k \sin\theta_1}\right)^{\frac{a}{2}}} \right] \left[ a \frac{\sin\left(\frac{k_x - k \sin\theta_1}{k_x - k \sin\theta_1}\right)^{\frac{a}{2}}}{\left(\frac{k_x - k \sin\theta_1}{k_x - k \sin\theta_1}\right)^{\frac{a}{2}}} \right] dk_x \right|^2 \quad (46)$$

Equations (45) and (46) are normalized with respect to wavelength. These normalized equations are then evaluated numerically and compared with MOM solutions. The bistatic solutions for a two wavelength strip are shown in figures 3, 4, and 5 for incidence angles of  $0^\circ$ ,  $-30^\circ$ , and  $-45^\circ$ , respectively. Figures 6 and 7 compare the monostatic solutions for two and three wavelength strips, respectively. As evident from these figures, the Fourier transform technique accurately predicts the null and

peak locations in the scattering width patterns. The predicted levels agree quite well with the MOM predictions in the specular regions but tend to be lower than the MOM predictions for other angles.

## CONCLUDING REMARKS

This paper introduces a different approach for predicting the scattering widths for strips. The technique is based on Fourier transformations for determining the linear current density flowing on the strip. However, it has been shown that there is no need to solve for the linear current density explicitly, thus reducing the computational time required to obtain scattering width patterns. On the other hand, the MOM technique requires explicit solutions for the linear current densities which can be time consuming, particularly for monostatic scattering widths.

The technique presented in this paper predicts quite well the shapes of the scattering widths but not their absolute levels for all angles. Methods of improving the accuracy of this technique will be investigated in future work.

## REFERENCES

1. Harrington, R.F.: *Time-Harmonic Electromagnetic Fields*, McGraw-Hill Book Company, 1961.
2. Balanis, C.A.: *Antenna Theory: Analysis and Design*, Wiley, 1982.
3. Keller, J.B.: "Geometrical theory of diffraction," *J. Opt. Soc. Amer.*, vol. 52, no. 2, February 1962.
4. Kouyoumjian, R.G. and Pathak, P.H.: "A uniform geometrical theory of diffraction for an edge in a perfectly conducting surface," *Proc.IEEE*, vol. 62, no. 11, November 1974.
5. Balanis, C.A.: *Advanced Engineering Electromagnetics*, Wiley, 1989.
6. Stutzman, W.L. and Thiele, G.A.: *Antenna Theory and Design*, Wiley, 1981.

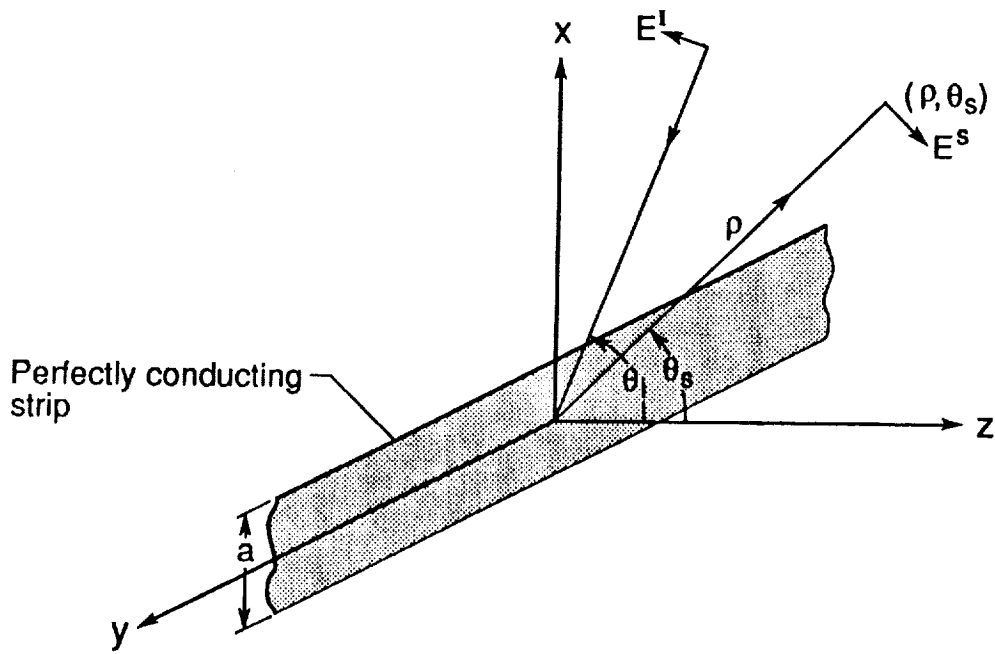


Figure 1. Strip geometry

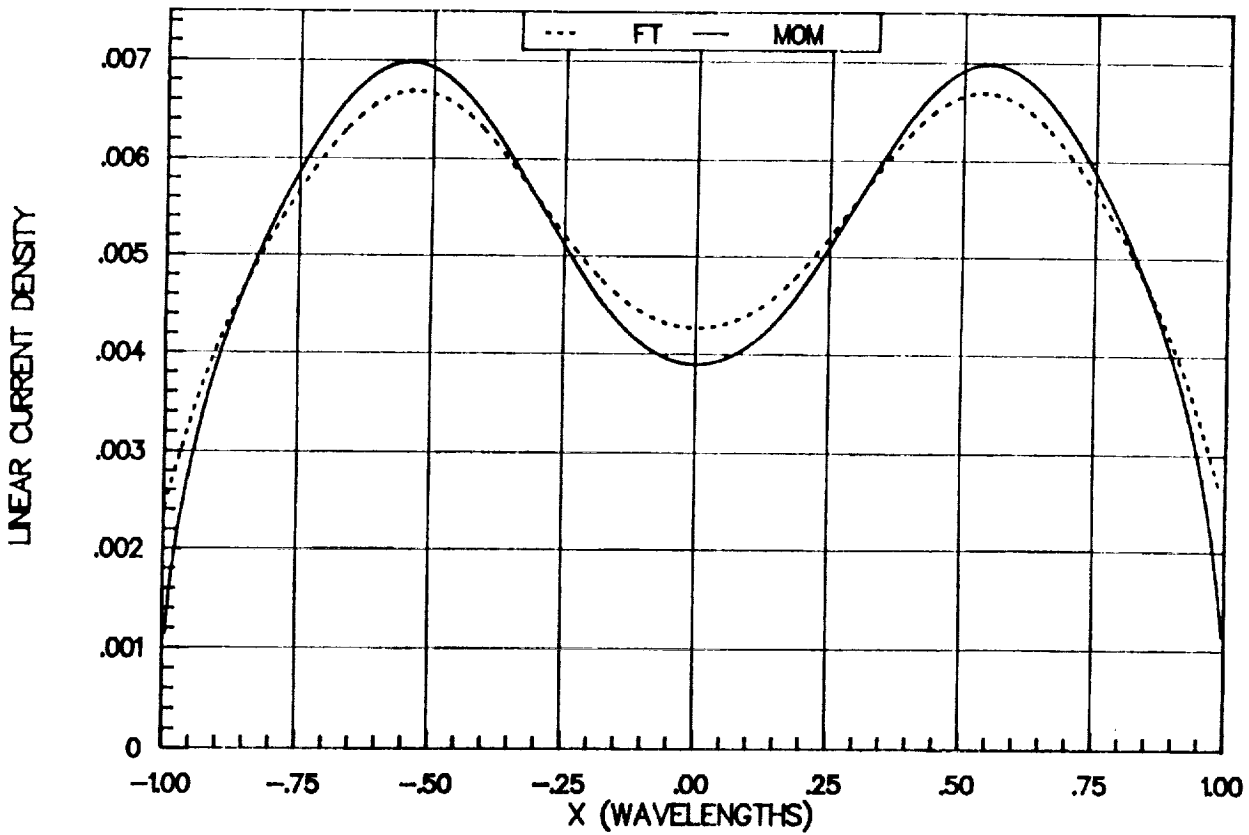


Figure 2. Comparison of linear current densities induced on a two wavelength strip at normal incidence



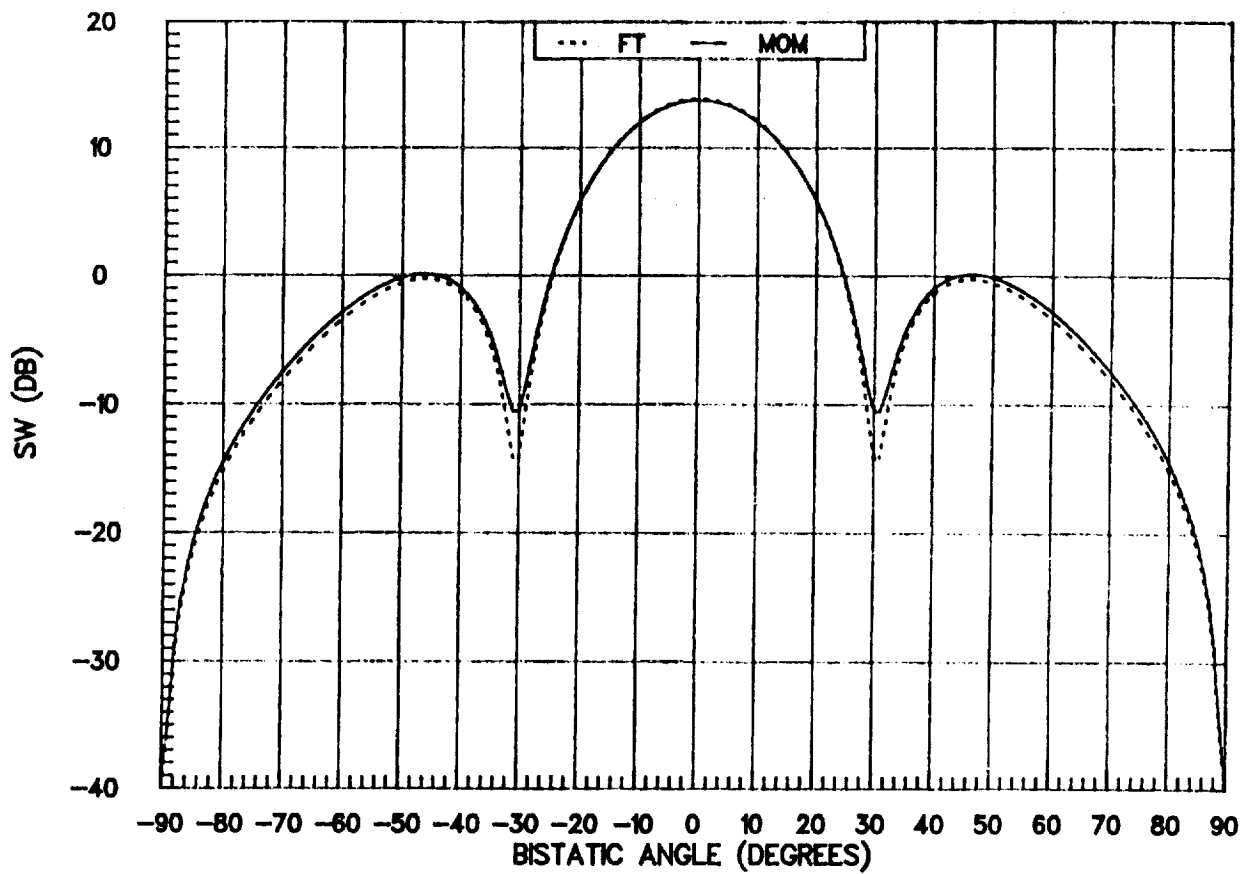


Figure 3. Comparison of TE bistatic scattering widths of a two wavelength strip at normal incidence

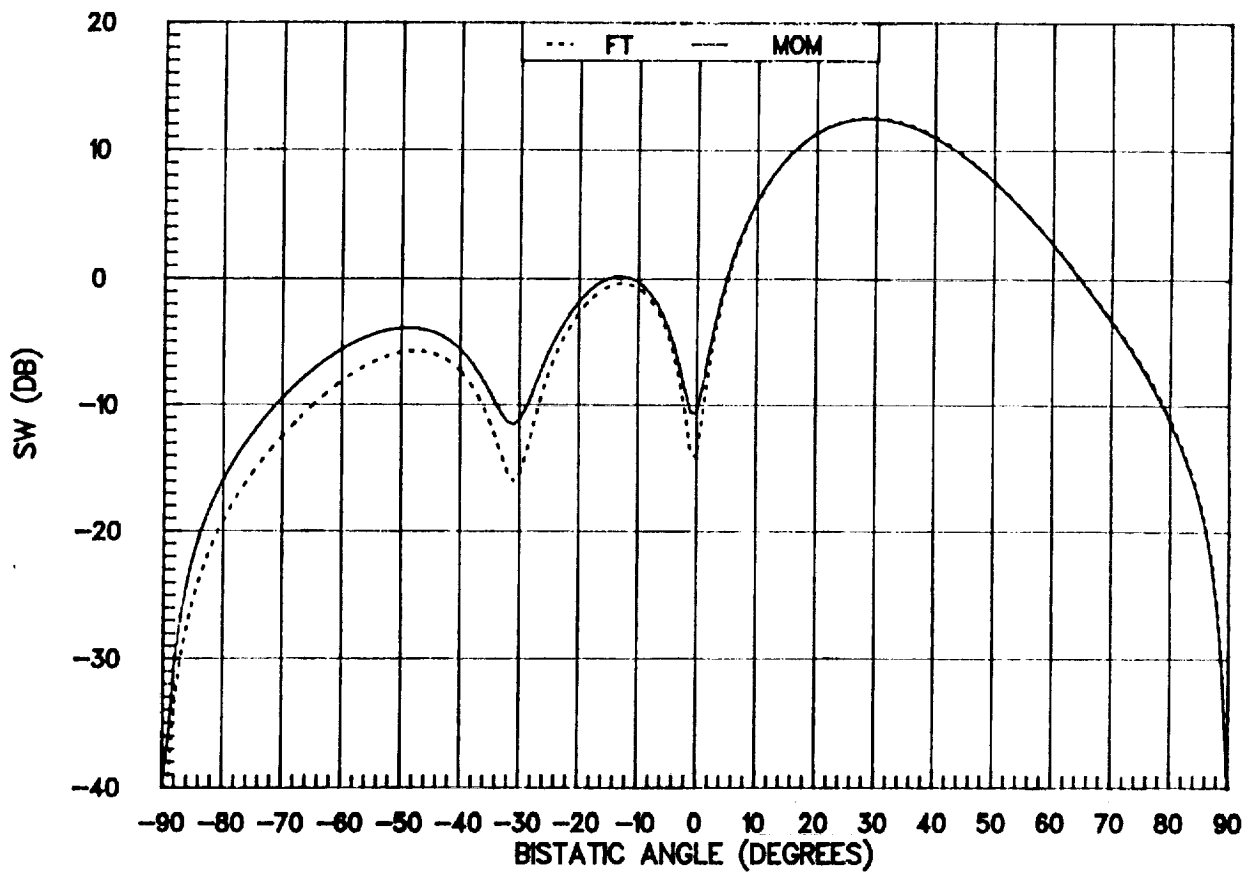


Figure 4. Comparison of TE bistatic scattering widths of a two wavelength strip at -30 degrees incidence

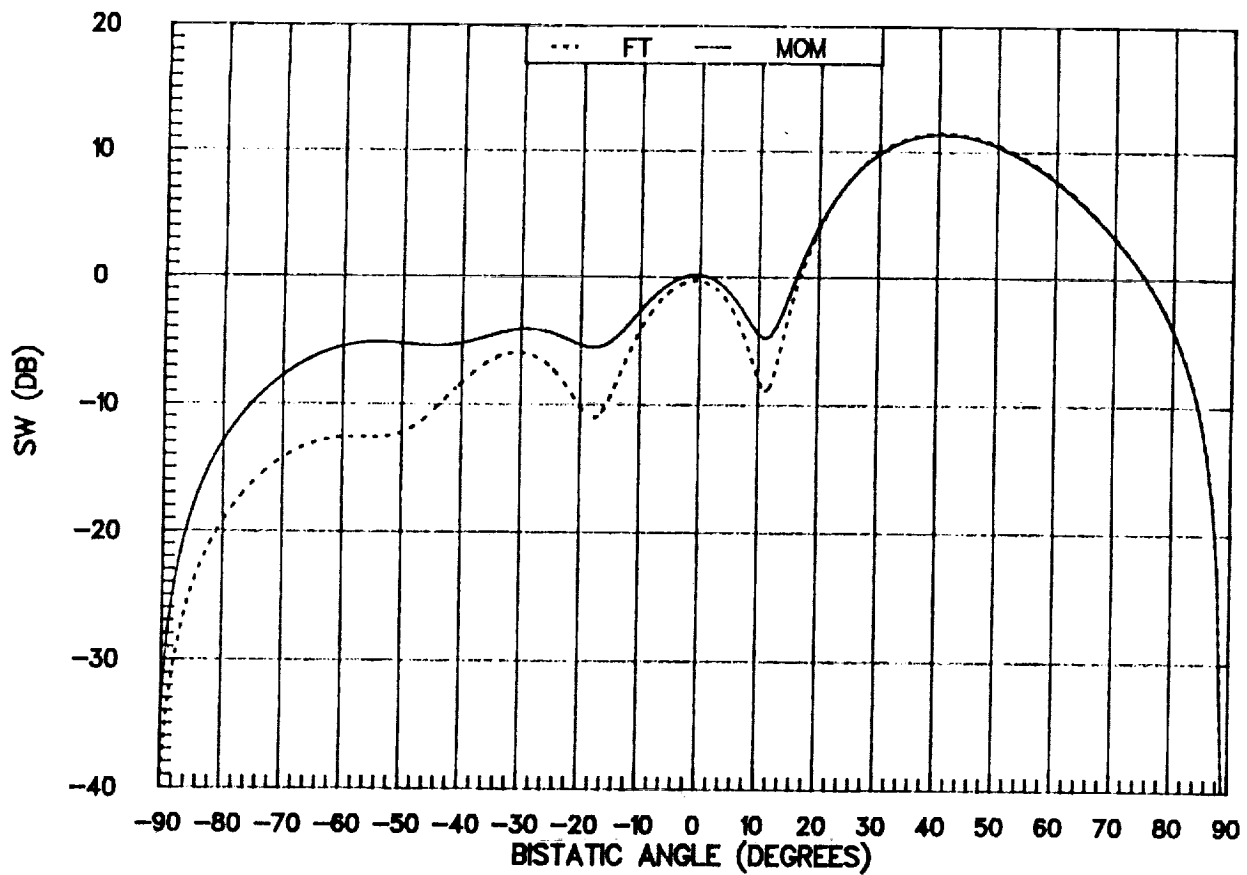


Figure 5. Comparison of TE bistatic scattering widths of a two wavelength strip at -45 degree incidence

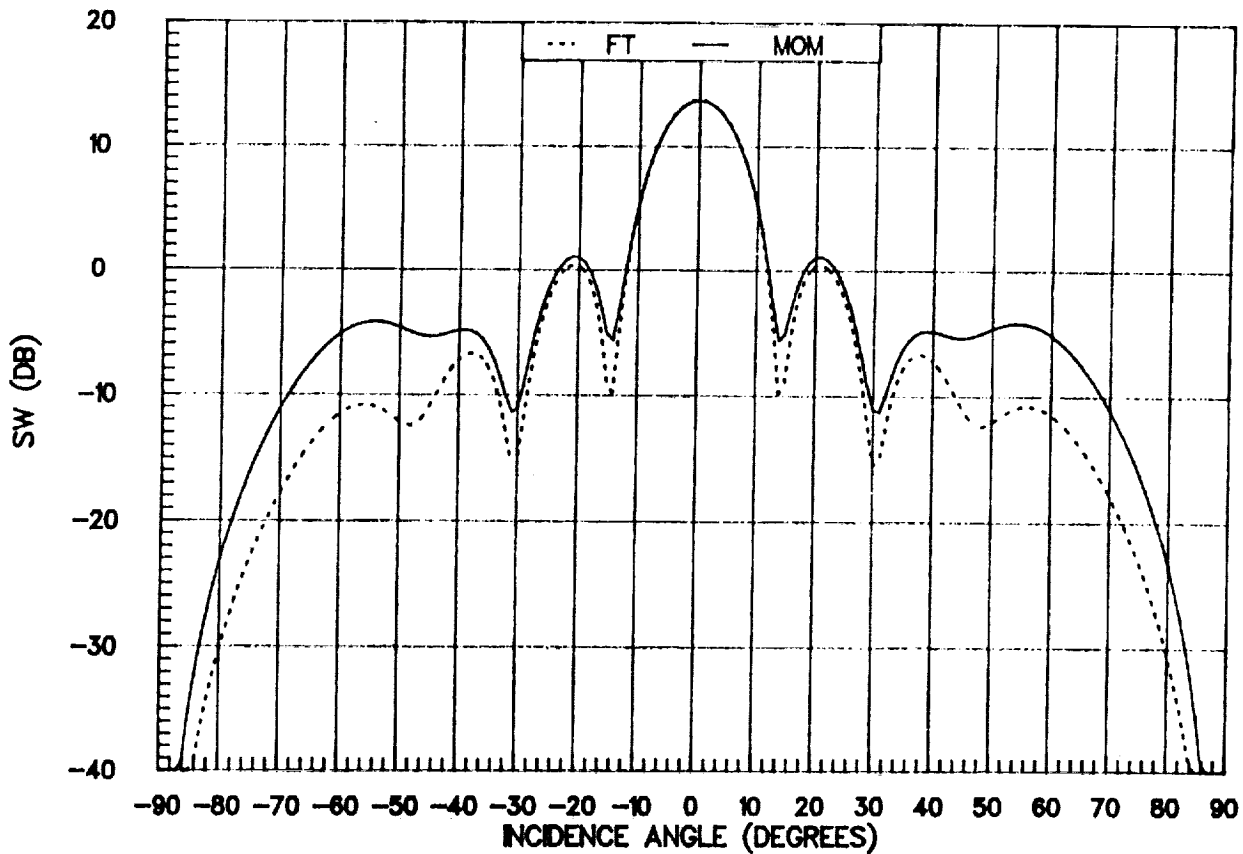


Figure 6. Comparison of TE monostatic scattering widths for a two wavelength strip

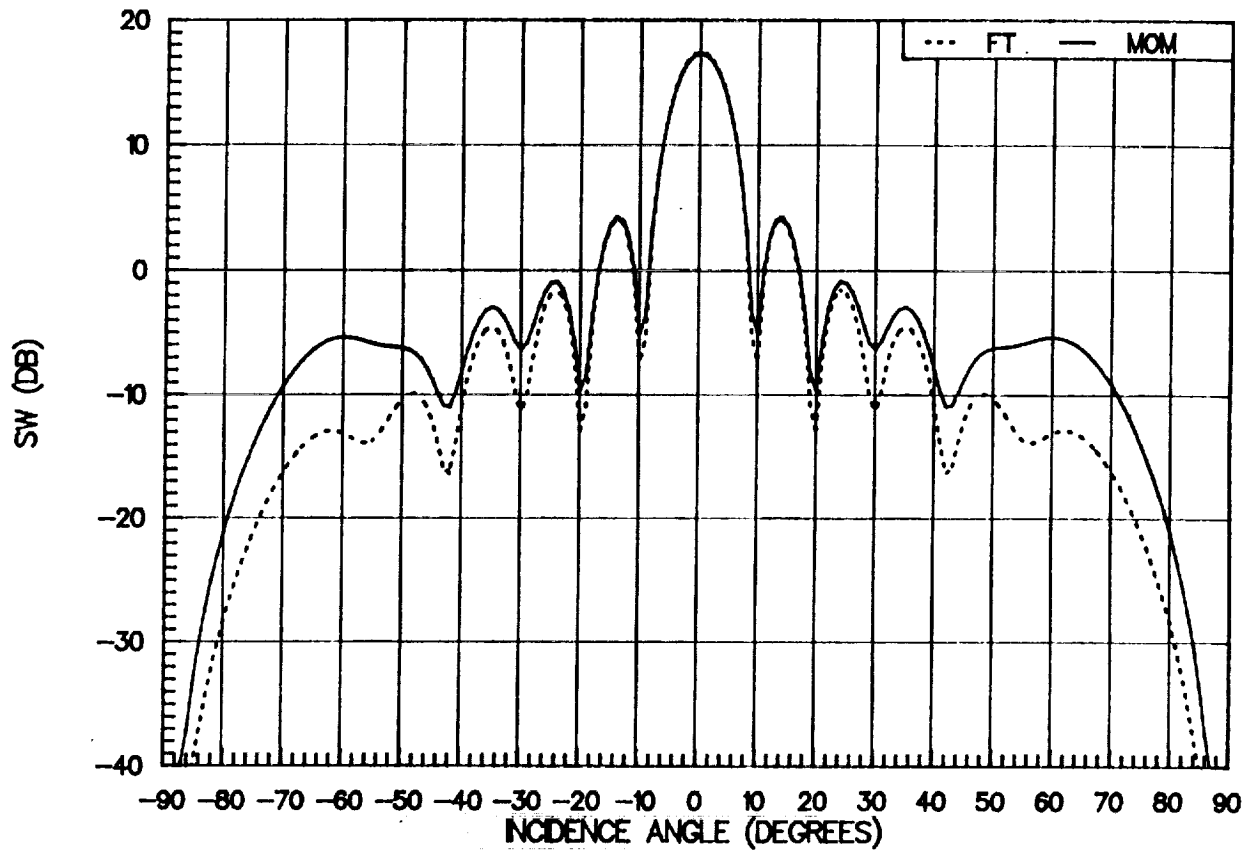


Figure 7. Comparison of TE monostatic scattering widths for a three wavelength strip



# Report Documentation Page

1. Report No.  NASA TM-102729		2. Government Accession No.		3. Recipient's Catalog No.	
4. Title and Subtitle  Transverse Electric Scattering Widths for Strips - Fourier Transform Technique				5. Report Date  June 1991	
				6. Performing Organization Code	
7. Author(s)  C. R. Cockrell S. D. Harrah F. B. Beck				8. Performing Organization Report No.	
				10. Work Unit No.  505-64-70-01	
9. Performing Organization Name and Address  NASA Langley Research Center Hampton, Virginia 23665-5225				11. Contract or Grant No.	
				13. Type of Report and Period Covered  Technical Memorandum	
12. Sponsoring Agency Name and Address  National Aeronautics and Space Administration Washington, DC 20546-0001				14. Sponsoring Agency Code	
				15. Supplementary Notes	
16. Abstract A technique which is based on Fourier transformations is introduced for predicting scattering widths. For a strip it is shown that explicit determination of the linear current density is not necessary for both bistatic and monostatic scattering width calculations. Comparisons of the predictions of the technique in this paper are made with the integral equation (IE) technique predictions, which do require explicit evaluations of linear current densities.					
17. Key Words (Suggested by Author(s)) strip Fourier transform scattering width			18. Distribution Statement  unclassified - unlimited  subject category 32		
19. Security Classif. (of this report)  unclassified		20. Security Classif. (of this page)  unclassified		21. No. of pages  18	22. Price  A03